


## Enhancement of Heat Transfer and Fluid Flow Characteristics in an Elliptical Tube with a Twisted Tube Section and Twisted Tape Inserts: A Numerical Investigation



Hadi O. Basher 

Mechanical Engineering Department, College of Engineering, Wasit University, Al-kut-Wasit 52001, Iraq

Corresponding Author Email: [hadi@uowasit.edu.iq](mailto:hadi@uowasit.edu.iq)

Copyright: ©2024 The author. This article is published by IIETA and is licensed under the CC BY 4.0 license (<http://creativecommons.org/licenses/by/4.0/>).

<https://doi.org/10.18280/ijht.420437>

### ABSTRACT

**Received:** 5 April 2024

**Revised:** 25 June 2024

**Accepted:** 10 July 2024

**Available online:** 31 August 2024

#### **Keywords:**

*heat transfer, elliptical tube, twisted tube, twisted tape inserts, Nusselt number, performance evaluation criterion (PEC)*

This computational study explores the thermal and hydrodynamic behavior of a novel heat exchanger tube design combining a twisted elliptical tube section with twisted tape inserts placed before a regular flat elliptical tube section. The geometric model is analyzed using ANSYS FLUENT software, which applies a finite volume approach and a  $k-\omega$  SST turbulence model. The results indicate that including a twisted section and vortex-induced inserts improves heat transfer efficiency compared to a standard elliptical tube that does not have these features. Notably, the Nusselt number is augmented by 26.36% for the elliptical plain tube with twisted tube section coupled with twisted tape inserts at pitch=0.05 m, and 10.9% for the elliptical plain tube with twisted tube section at pitch=0.05 m, relative to the elliptical plain tube configuration. The smaller twist pitch of 0.025 m is found to yield the highest Nusselt number and performance evaluation criterion (PEC). The configuration with the tightest pitch of 0.025 m shows a higher heat transfer performance, resulting in the highest Nusselt number and PEC. Specifically, this design achieves a significant 67.3% increase in Nusselt number compared to the standard channel, along with a peak PEC value of 1.128. But, this significant thermal improvement comes at the cost of increased flow resistance. The friction factor increases by 46.56% with both the twisted section and vortex generators, and by 14.62% with the twisted section only, compared to the basic smooth channel design.

## 1. INTRODUCTION

Compact heat exchangers are widely utilized across a variety of industrial domains, such as chemical engineering, power generation, waste heat recovery, and air conditioning [1]. The contemporary global focus on energy preservation, which has been amplified by the escalating scarcity of energy sources, has experienced a notable surge in recent times [2]. This increased consciousness has triggered extensive academic investigations that are specifically aimed at improving convective heat transfer. The primary goal of this research is to improve heat transfer efficiency with reduction of pressure loss at the same time. Achieving this accurate balance is important to enhancing both the compactness and overall performance of heat exchangers, and meeting the growing demand for energy efficient systems. Continuous improvement in convective heat transfer within compact heat exchangers is essential to meet the evolving requirements of diverse industrial applications. This approach reflects the broader trend towards developing more efficient thermal management solutions that can deliver superior performance in smaller packages, thus contributing to overall energy conservation and system optimization across various sectors.

Elliptical tubes are extensively utilized in heat exchanger applications, particularly in cross-flow configurations, due to their advantages [3]. When compared to circular tubes,

Elliptical tubes possess a streamlined design that enhances the efficiency of fluid flow within the interstitial space [4]. This characteristic results in reduced pressure losses and more favorable velocity distributions, thereby minimizing the occurrence of stagnant flow regions.

However, the primary drawback of conventional elliptical tubes lies in their limited ability to sufficiently enhance heat transfer efficiency and fluid mixing to keep pace with today's industrial development. Standard elliptical tubes have limitations in generating sufficient turbulence and promoting fluid mixing. This limitation results in reduced interaction between the liquid and the tube walls, causing non-uniform heat distribution and relatively low heat transfer rates [5]. On the other hand, twisted elliptical tubes, with their helical or twisted configuration can overcome these limitations by promoting enhanced fluid mixing, increased turbulence, disrupted flow patterns, and extended contact between the fluid and tube walls [6]. Twisted elliptical tubes, in contrast to conventionally smooth tubes, alter the linear flow pattern within them to a spiral flow, thereby generating a secondary flow which is vertical to the primary flow direction [7].

In the realm of heat transfer, researchers are constantly studying innovative technique to improve the performance of heat exchangers. One promising approach involves utilizing twisted tubes and twisted tapes to produce swirl flow and boost thermal rates. By introducing a twist to the tube or tape, a

swirling motion is created within the fluid, resulting in increased turbulence and better mixing [7]. Improved flow dynamics facilitate more efficient heat exchange between the fluid and the surfaces of both the channel and vortex generator. Research has shown that the combination of a helically twisted channel section and internal vortex generators results in much higher heat transfer rates compared to conventional circular tubes or twisted tubes without inserts.

Elliptical tubes have garnered significant research interest due to their unique fluid flow and heat transfer characteristics than the conventional circular tubes. The elliptical cross-section geometry has been demonstrated to influence the development of secondary flows and alter the velocity and thermal boundary layer profiles. Specifically, studies have shown that elliptical tubes can promote the formation of two counter-rotating vortices in the tube cross-section, leading to improved fluid mixing and disruption of the thermal boundary layer [8, 9]. Vortex generation is the result of an irregular cross section, which creates variations in the centrifugal forces acting on the fluid. It has also been observed that the ellipse shape enhances heat transfer efficiency by creating regions with high heat transfer coefficients near the major axis of the ellipse, in contrast to low coefficients along the minor axis [10]. yet, the magnitude of these effects depends on variables including the aspect ratios of the ellipse, as well as the class of fluid motion and the scale of turbulence [11]. By exploiting their distinct circulation and heat exchange features, Elliptical tubes have shown potential in diverse temperature regulation system applications. This research seeks to develop an innovative hybrid design that combines the advantages of spirally twisted elliptical channels with vortex-generating internal inserts. But, it is important to consider an increase in pressure loss when performing optimization. Hence, careful optimization is required to achieve the ideal balance between enhanced heat exchange and resulting pressure drop penalties.

Indurain et al. [12] analyzed short-length twisted tube configurations that induce swirling flows. The results showed that the twisted tube with an elliptical cross-section (STE) improved heat transfer by 22% to 90% compared to a plain tube. However, this improvement came at the cost of a higher pressure drop of 63% to 129%. Zhao et al. [13] discovered that twisted elliptical tubes significantly enhance heat transfer but also increase flow resistance. Compared with straight cylindrical channels, the total heat transfer capacity of twisted elliptical channels is 1.68 times larger, and the specific area heat transfer capacity shows an increase of 1.43 times. For twisted elliptical channels with a spiral pitch of 200 mm, the TCF is approximately 1.596. These data highlight the significant thermal benefits of twisted elliptical geometries, while also recognizing the trade-off with increased flow resistance. Also, the employ of twisted elliptical tubes results in a rise in the pressure drop of LBE (Lead-Bismuth Eutectic) by approximately 30.4%. Alempour et al. [7] revealed that altering the conduit's profile from round to oval-shaped and diminishing the dimensional ratio can result in heightened resistance to the flow and thermal exchange. Particularly, within an elliptical channel possessing a shape factor of 1.65, a twist pitch of 0.4 produced in a 5% enhancement in heat transfer than the smooth tube. Similarly, a twist pitch of 0.2 led to a significant 20% enhancement in convection. Further reducing the twist pitch to 0.1 resulted in a substantial 30% increase in heat transfer. Cheng et al. [5] performed a computational study on helically twisted channels with various cross-sectional geometries to examine their thermal

and fluid dynamic properties. The results revealed that the twisted channels showed an improvement in heat transfer performance compared to standard smooth channels, but this improvement came with the disadvantage of higher pressure loss. Particularly noteworthy was the twisted pentagon tube, which achieved a high-performance Evaluation Criterion (PEC) of 2.69 at a twist pitch ratio of 0.17.

Luo et al. [14] discovered that incorporating a twisted oval tube in an innovative annular tube configuration lead to significant improvements in heat transfer compared to a setup with two straight oval tubes. The outcomes of the study indicate that the twisted tube configuration achieves a maximum Nusselt number 116% higher than the straight tube, indicating a significant improvement in heat transfer. This enhancement is accompanied by a relatively moderate 46% increase in the friction factor. The thermal performance factor peaks at an impressive value of 1.9, indicating a proper balance between heat transfer gains and flow resistance penalties.

Recently, tape inserts were used in different shapes for improve heat transfer rate. Samruaisin et al. [11] investigated the heat transfer rate and friction loss performance of a combination of twisted pipes and twisted tapes. The findings showed that, at a twist ratio of 2.0, the heat transfer rate was 70.4% higher compared to using the twisted pipe alone and 172% higher than using a smooth pipe. However, it is important to note that the friction factor increased by 276% compared to using the twisted tube alone and was 12 times higher than using a smooth tube. Mushatet et al. [15] studied different tapered shapes of twisted tape within a heated tube to determine the most effective setup for enhancing thermal performance. The findings of the study demonstrated significant improvements in heat transfer: a numerical Nusselt number increase of up to 100%. Additionally, the friction factor exhibited a substantial rise, with numerical outcomes indicating a maximum increase of 226%. Regarding the thermal performance factor, the numerical analysis suggested a higher value of 1.37. Tusar et al. [16] employed computational fluid dynamics (CFD) using ANSYS FLUENT to perform a comprehensive three-dimensional analysis of heat and mass transfer. The results indicated that for a twist ratio of 3.46, Nusselt numbers experienced an increase ranging from 20% to 62%. However, it is important to note that friction factors exhibited a substantial rise of 185% to 245%. The thermal performance factor was observed to vary between 0.9 and 1.2, reflecting the overall efficiency of the heat transfer process. Outokesh et al. [17] conducted a numerical analysis to investigate the effects of curved twisted tapes on turbulent fluid flow and heat transfer in a circular tube. The study revealed noteworthy improvements in heat transfer performance. Specifically, curved twisted tapes with a height of 7mm demonstrated an impressive 35% increase in thermal performance compared to the base case. Similarly, curved twisted tapes with a height of 5mm exhibited a substantial improvement of 30%. Alzahrani and Usman [18] conducted a computational fluid dynamics (CFD) study to study the effect of internal twisted band configurations on heat transfer and pressure loss. The research yielded important results. It is worth noting that the use of full-length twisted tapes with a pitch-to-diameter (p/d) ratio of 2.7 resulted in a significant improvement of 28% in heat transfer. But, it is important to note that this improvement in thermal performance came at the cost of a significant 102.8% increase in pressure drop.

Based on the above-mentioned remarks, previous studies

used twisted tubes and twisted tape inserts to investigate their performance for different fluids, cross-section shapes, twist pitch lengths, and Reynolds numbers. Most previous studies have demonstrated that the utilization of twisted tubes and twisted tape inserts results in enhanced heat transfer rates compared to flat tubes, albeit at the expense of increased pressure.

This study aims to take a look at a new type of heat exchanger tube design that has not been explored before to the author's knowledge. The research focuses on analyzing the thermal and fluid flow performance of a hybrid tube setup. This unique design combines a twisted elliptical tube section, known for creating swirling flows and improving heat transfer, with twisted tape inserts placed before a regular flat elliptical tube section.

The goal is to see if this hybrid configuration can achieve maximum heat transfer rates than the fully twisted elliptical tube design, while also reducing the associated pressure drop penalties. The investigation examined the overall effectiveness of this elliptical tube with twisted tape inserts using specific criteria that balance the need for better heat transfer and lower pressure drop.

The motivation behind this new approach comes from the need to develop heat exchanger geometries that can optimize these two often conflicting objectives. In many industrial applications, both enhancing heat transfer and managing pressure are extremely important.

## 2. NUMERICAL APPROACH

The governing equations of the mathematical model were solved numerically using the finite volume method (FVM), as carried out in ANSYS Fluent software. This approach separates the equations across control volumes, transforming the partial differential equations into a system of algebraic equations. A segregated solver approach was used, solving the equations sequentially.

The convective components of the equations were separated using a second-order upwind scheme, which was chosen to enhance its accuracy and stability. For diffuse terms, a second-order central differentiation scheme was applied. To manage the pressure-velocity coupling in the incompressible flow scenario, the SIMPLE (semi-implicit method for pressure-related equations) algorithm was used.

The solution procedure involved initializing the flow field, then iteratively:

1. Solving the momentum equations for updated velocities using the current pressure field and previously updated velocities.
2. Deriving the pressure correction equation from continuity and updated velocities, and correcting the pressure field.
3. Using the corrected pressure to update the velocities, ensuring mass conservation.
4. Solving the energy equation for temperature using the updated velocities and pressures. This process continued until residuals fell below specified thresholds (typically  $10^{-6}$  for energy,  $10^{-4}$  for others).

Boundary conditions were applied at inlets (velocity profile, temperature), outlets (pressure outlet), and walls (no-slip, constant heat flux). For turbulent cases, the  $k-\omega$  SST model provided closure by solving transport equations for turbulent kinetic energy ( $k$ ) and specific dissipation rate ( $\omega$ ), coupled

with the momentum and energy equations [19].

Solution acceleration techniques included CFL ramping (gradually increasing time-step size), relaxation factors (controlling variable updates between iterations), and a pseudo-transient approach (marching in pseudo-time for initial solutions far from convergence).

Grid independence studies and validation against experiments ensured solution accuracy. Discretization schemes, boundary conditions, and turbulence models were selected based on the problem requirements and desired accuracy/efficiency trade-offs.

### 2.1 Physical model

In this study, the elliptical tubes with twisted tubes having twisted tape geometrical features are shown in Figure 1. The entrance zone ( $S_{in}$ ), exit zone ( $S_{out}$ ), and heat exchange segment ( $S$ ) are smooth and straight elliptical tubes. Fluid movement continues along the longitudinal axis in the Cartesian frame. Heat exchange sector ( $S$ ) extends 200 mm. In addition, the twisted tube ( $S_t$ ) is 50 mm. To ensure full flow development and prevent possible backflow, the length of the entry zone  $S_{in}$  and the length of the exit zone  $S_{out}$  are 5-10 times the characteristic dimension of the twisted channel.

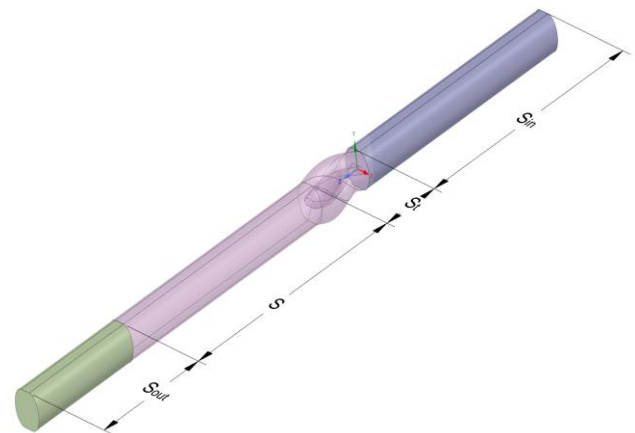


**Figure 1.** Schematic view of smooth elliptical tube joined with elliptical twisted tube and twisted tape insert

### 2.2 Mesh description

This study presents a thorough numerical investigation of the fluid dynamics and heat transfer phenomena occurring inside a tube. A polyhedral mesh configuration, as depicted in Figure 2, is utilized to discretize the tube geometry, facilitating the precise depiction of intricate flow patterns and thermal boundary layer characteristics. Inflation layers are strategically incorporated near the tube wall to effectively resolve both the velocity and thermal boundary layers. The non-dimensional  $y^+$  parameter is diligently regulated to sustain grid reliability, with values ranging from 0.27, 0.3 and 0.25 at  $Re=5000$  and 0.9132, 0.94586, and 1.08642 at  $Re=20000$  for the smooth elliptical tubes, smooth elliptical tube joined with twisted elliptical tubes without twisted tape and smooth elliptical tube joined with twisted elliptical tubes and twisted tape respectively as shown in Figure 3. The closest node is positioned at a distance of 0.1 mm from the tube wall to precisely capture the velocity boundary layer.

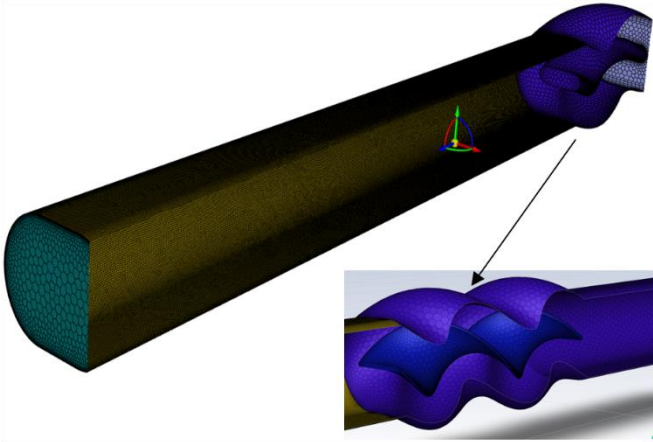


**Figure 2.** Detail view of the computational mesh of twisted square tube

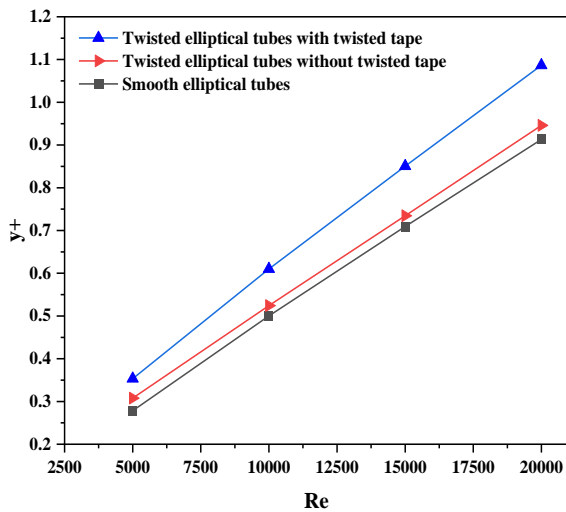


**Figure 3.** The non-dimensional  $y^+$  parameter for different types of tubes

### 2.2.1 Grid Independence test (GIT)

This research aims to assess the influence of varying grid sizes on the precision of numerical outcomes. Numerical studies were performed utilizing twisted elliptical tubes with twisted tape at a Reynolds number of 5000. In the numerical study, the mesh density was gradually increased to achieve satisfactory convergence between the computational results of the two most recent mesh configurations. The calculated data, including Nusselt number and friction loss values, are shown in Table 1 and Figure 4. Table 1 and Figure 4 show the decreasing variance in Nusselt number and friction loss measurements as the total number of mesh cells increases for twisted elliptical channels included twisted tape. The results indicate that the difference in Nusselt numbers and friction factors remains less than 1% at the number of elements 421,151 and 1,107,315. This indicates that further increments in the number of grid elements will not significantly affect the numerical results. Consequently, we select a grid system comprising 421151 cells for the simulations. Additionally, comparable mesh independence analyses were performed for additional configurations.

### 2.2.2 Validation

To ensure the trustworthiness and accuracy of the numerical outcomes, an evaluation was conducted by comparing the

Nusselt numbers and friction factors derived from the elliptical spiral tube (TOT) model in this study with the experimental results documented by Talebi and Lalgani [20] as shown in Figure 5.

**Table 1.** Variation in the average Nusselt number as a function of the grid size

Total Element Number	$Nu$	Relative Error	$f$	Relative Error
95015	68.9	-----	0.01461	-----
165424	69.4	0.00768	0.0145	0.0042
295362	70.5	0.01597	0.0145	0.0019
421151	70.9	0.00571	0.0144	0.0032
1107315	71.1	0.00165	0.0144	0.0021

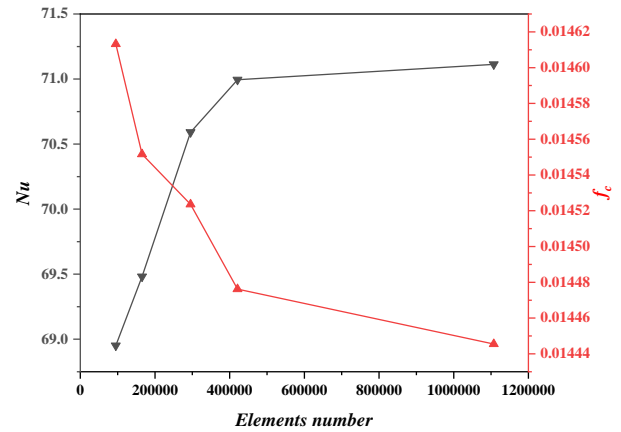


**Figure 4.** Convergence of Nusselt number ( $Nu$ ) and friction factor ( $f_c$ ) with elements number

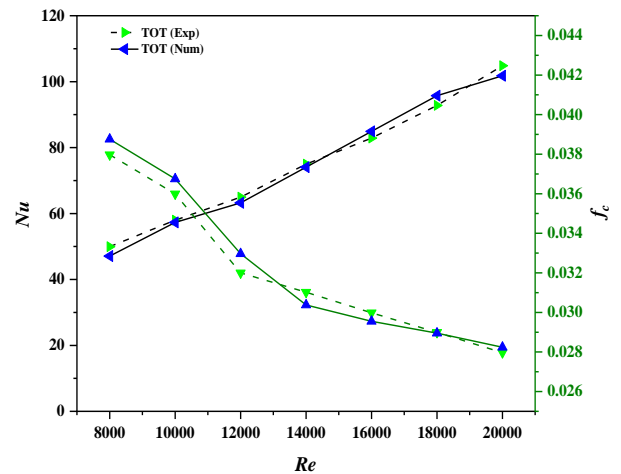


**Figure 5.** Comparison of Nusselt number and friction factor for turbulence models with experimental data [20]

The comparative study indicates that there are small differences between the experimental measurements and the computational results of this research. For a Reynolds number of 8000, the largest deviation in heat transfer performance, as measured by Nusselt number, was observed in the helically twisted square channel, reaching 6% in magnitude, while the minimum discrepancy is 1.3% at  $Re=14000$ . Similarly, the friction factor exhibits a discrepancy ranging from 2.81% at  $Re=8000$  to 1.72% at  $Re=18000$ . These disparities can be attributed to the inherent distinctions between the experimental and numerical methodologies. Specifically, the

boundary conditions of the computational model may not accurately reflect those used in the experimental setting, and the experimental study may contain inherent measurement uncertainties. Despite these potential discrepancies, the overall alignment between experimental results and numerical predictions validates the current simulation approach to accurately predict thermodynamic and fluid behaviors in helically twisted channels.

### 2.3 Boundary conditions

The computational analysis conducted using Ansys Fluent focused on examining the characteristics of an incompressible Newtonian fluid flowing steadily within the elliptical tube, twisted elliptical tubes, and twisted elliptical tubes that were modified with twisted tape geometries. The assumption of water's incompressibility guided the careful selection and application of specific boundary conditions to accurately simulate real-world flow scenarios. At the inlet of the computational domain, the flow profile was imposed to be fully developed, mirroring established flow conditions. A fixed temperature of 300 K was prescribed at the inlet to represent the thermal state of the incoming water.

Within the test section of the tube, a constant heat flux boundary condition was applied to simulate the scenario where the tube experiences a consistent heat input. This special boundary condition facilitated the exploration of heat transfer properties within the system, which assumes incompressible flow behaviour. The adoption of these demarcation conditions aims to reflect the original scenarios prevailing in practical applications, allowing a comprehensive examination of the thermal transport properties and fluid dynamics within the incompressible domain of twisted elliptical tubes reinforced with twisted band configurations.

### 2.4 Governing equations

The study focused on the analysis of forced convection heat transfer inside the ducts, taking into account the previously mentioned assumptions and limitations. In computational fluid dynamics (CFD), fluid motion is generally described by basic mathematical formulas, often as partial differential equations known as governing equations. These equations dictate the specific process under investigation and are vital in the modeling process. Choosing and applying these governing equations accurately is a pivotal step in modeling, because it involves representing an idealized version of the physical problem based on these equations [21].

Continuity equation:

The continuity equation for an incompressible fluid flow can be derived by applying the mass conservation principle to a control volume. The detailed derivation is as follows:

1. Consider a fixed control volume (CV) with a surface area A and fluid flowing through it.
2. The rate of mass accumulation within the CV=(Rate of mass entering the CV) - (Rate of mass leaving the CV).
3. Let  $\rho$  be the fluid density, and  $u, v, w$  be the velocity components in  $x, y, z$  directions respectively.
4. The rate of mass entering the CV through the  $x$ -face= $\rho u dydz$ .
5. Rate of mass leaving the CV through the opposite  $x$  - face =  $\rho u dydz + \left(\frac{\partial(\rho u)}{\partial x}\right) dx dydz$ .
6. Applying similar expressions for the  $y$  and  $z$  faces, and setting the rate of mass accumulation to zero for an

incompressible flow, we get  $\frac{\partial(\rho u)}{\partial x} + \frac{\partial(\rho v)}{\partial y} + \frac{\partial(\rho w)}{\partial z} = 0$ .

7. For an incompressible flow,  $\rho$  is constant, so the above equation reduces to  $\frac{\partial u}{\partial x} + \frac{\partial v}{\partial y} + \frac{\partial w}{\partial z} = 0$ .

This is the continuity equation for an incompressible fluid flow in Cartesian coordinates.

Navier-Stokes equations:

The Navier-Stokes equations for momentum conservation can be derived by applying Newton's second law of motion to a fluid element and incorporating the viscous stress terms.

X-momentum equation:

1. Consider a fluid element of dimensions  $dx, dy, dz$ , with sides parallel to  $x, y, z$  coordinate axes.

2. The forces acting on the fluid element in the  $x$ -direction are:

- Surface forces (pressure and viscous forces) on  $x$ -faces
- Surface forces (viscous forces only) on  $y$  and  $z$  faces
- Body force (e.g. gravity)

3. Applying Newton's second law in the  $x$ -direction:

$$\rho \left(\frac{du}{dt}\right) dx dy dz = \left[p - \left(p + \frac{\partial p}{\partial x} dx\right)\right] dy dz \text{ (pressure forces)}$$

$$+ \left[\tau_{xx} - \left(\tau_{xx} + \frac{\partial \tau_{xx}}{\partial x} dx\right)\right] dy dz \text{ (x-direction viscous forces)}$$

$$+ \left[\tau_{yx} - \left(\tau_{yx} + \frac{\partial \tau_{yx}}{\partial y} dy\right)\right] dx dz \text{ (y-direction viscous forces)}$$

$$+ \left[\tau_{zx} - \left(\tau_{zx} + \frac{\partial \tau_{zx}}{\partial z} dz\right)\right] dx dy \text{ (z-direction viscous forces)}$$

$$+ \rho f_x dx dy dz \text{ (body force)}$$

4. Canceling out terms, dividing through by  $dx dy dz$ , and using constitutive relations for Newtonian fluids, we get the x-momentum Navier-Stokes equation:

$$\rho \left(\frac{\partial u}{\partial t} + \frac{u \partial u}{\partial x} + \frac{v \partial u}{\partial y} + \frac{w \partial u}{\partial z}\right) = -\frac{\partial p}{\partial x} + \mu \left(\frac{\partial^2 u}{\partial x^2} + \frac{\partial^2 u}{\partial y^2} + \frac{\partial^2 u}{\partial z^2}\right) + \rho f_x$$

The  $y$  and  $z$  momentum equations can be derived similarly.

#### Energy Equation:

The energy equation can be derived by applying the first law of thermodynamics to a fluid element and considering various modes of energy transfer.

1. Consider a fluid element of volume  $V=dx dy dz$ , surface area A.

2. The rate of change of energy of the fluid element = Net rate of heat addition + Net rate of work done on the element

3. Using Fourier's law for heat conduction and the definition of viscous dissipation, we get:

$$\rho \left(\frac{\partial e}{\partial t} + \frac{u \partial e}{\partial x} + \frac{v \partial e}{\partial y} + \frac{w \partial e}{\partial z}\right) V =$$

$$- \left[q'' - \left(\frac{q + \partial q}{\partial x} dx\right)\right] dy dz \text{ (net heat conduction in x-dir)}$$

$$- \left[q' - \left(q' + \frac{\partial q'}{\partial y} dy\right)\right] dx dz \text{ (net heat conduction in y-dir)}$$

$$- \left[q'' - \left(\frac{q + \partial q}{\partial z} dz\right)\right] dx dy \text{ (net heat conduction in z-dir)}$$

$$\left[\tau_{xx} \left(\frac{\partial u}{\partial x}\right) + \tau_{yy} \left(\frac{\partial v}{\partial y}\right) + \tau_{zz} \left(\frac{\partial w}{\partial z}\right) \tau_{xy} \left(\frac{\partial u}{\partial y} + \frac{\partial v}{\partial x}\right) +$$

$$\tau_{xz} \left(\frac{\partial u}{\partial z} + \frac{\partial w}{\partial x}\right) + \tau_{yz} \left(\frac{\partial v}{\partial z} + \frac{\partial w}{\partial y}\right)\right] dx dy dz$$

(viscous dissipation)

4. Canceling terms, substituting Fourier's law, dividing by  $dx dy dz$ , and using  $e=cvT$ , we get the energy equation:

$$\rho cv \left(\frac{\partial T}{\partial t} + \frac{u \partial T}{\partial x} + \frac{v \partial T}{\partial y} + \frac{w \partial T}{\partial z}\right) = k \left(\frac{\partial^2 T}{\partial x^2} + \frac{\partial^2 T}{\partial y^2} + \frac{\partial^2 T}{\partial z^2}\right) + \mu 2 \left(\left(\frac{\partial u}{\partial x}\right)^2 + \left(\frac{\partial v}{\partial y}\right)^2 + \left(\frac{\partial w}{\partial z}\right)^2\right) + \left(\frac{\partial u}{\partial y} + \frac{\partial v}{\partial x}\right)^2 + \left(\frac{\partial u}{\partial z} + \frac{\partial w}{\partial x}\right)^2 + \left(\frac{\partial v}{\partial z} + \frac{\partial w}{\partial y}\right)^2$$

This is the energy equation for an incompressible fluid flow, accounting for conduction and viscous dissipation. Additional

source terms can be added as needed.

### 3. RESULT AND DISCUSSING

#### 3.1 Effect of twisted tube and twisted tape

##### 3.1.1 Flow patterns and temperature distribution

To gain deeper insight into the processes of increased heat transfer in elliptical tube with and without twisting tape inserts, the spatial patterns of flow paths, thermal gradients, and local Nusselt number have been visualized. Figure 6(a) illustrates the velocity streamline at Reynolds numbers of 5000 for different configurations: Smooth elliptical tube joined with elliptical twisted tube and twisted tape insert at pitch=0.05 m, smooth elliptical tube joined with twisted tube, and smooth tube alone. It can be observed from Figure 6(a) that the twisted tube, acting alone within the fluid flow system, instigates a series of significant alterations in the flow dynamics and temperature distribution along the tube walls. At the inlet, the short twisted tube section introduces a swirling and twisting motion in the fluid flow, imparting tangential velocity components and inducing secondary swirling flows and vortices within the tube. Consequently, the initially uniform velocity profile becomes distorted and twisted downstream of this section, leading to localized variations in flow velocity. This swirling motion enhances the mixing of the fluid, thereby redistributing thermal energy and affecting temperature distribution along the tube walls. As the flow progresses downstream, the swirling effect gradually diminishes due to viscous effects, although turbulence persists along the axial direction. Consequently, temperature gradients along the tube walls become more pronounced, with regions experiencing both elevated and reduced temperatures compared to the bulk fluid, resulting in a complex temperature distribution as shown in Figure 7(a).

When twisted tape inserts are combined with the twisted tube at the entrance of the smooth tube, the flow dynamics and temperature distribution undergo further modifications as shown in Figure 6(b) and Figure 7(b) respectively. The twisted tape introduces additional vortical motions and turbulence, further distorting the velocity profile and increasing mixing near the inlet region. This amplified mixing results in more pronounced temperature differences along the pipe walls, with localized hot zones and cold zones. The combined effect of the twisted tube and twisted tape inclusion perpetuates turbulent mixing downstream, culminating in a more uniform velocity profile compared to laminar flow conditions. As a result, temperature distribution along pipe walls becomes increasingly complex, with improved heat transfer properties and potential advances in thermal performance within the system.

The insertion of a twisted tube alone into a fluid flow system greatly affects the local Nusselt number at the wall. Firstly, the vortex and twisting motion generated by the twisted tube promotes mixing and redistribution of thermal energy within the flow. This generates a non-uniform temperature distribution along the tube walls, leading to variations in the local Nusselt number, as shown in Figure 8(a). Regions with intense vortices and turbulence show higher convective heat transfer coefficients, leading to higher heat transfer rates and increased local Nusselt numbers. On the other hand, regions with diminished eddy motion may exhibit lower convective heat transfer coefficients and hence lower local Nusselt

numbers. As the flow progresses downstream, the diminishing vortex effect reduces the intensity of temperature fluctuations, resulting in stabilization of the local Nusselt number along the pipe walls.

The combination of the twisted tape with the twisted tube at the smooth tube inlet further affects the local Nusselt number on the wall. The additional vortex motions and turbulence caused by the inclusion of the twisted strip intensify the mixing and heat transfer within the flow, leading to enhanced convective heat transfer coefficients and increased local Nusselt numbers near the inlet region, as shown in Figure 8(b). As the flow progresses downstream, sustained turbulent mixing from both the twisted tube and the twisted strip insert maintains high convective heat transfer coefficients, resulting in high local Nusselt numbers along the tube walls.

This combined effect results in improved heat transfer properties and higher overall thermal performance within the system. compare tubes with or without twisted tubes and tape inserts reveal significant variations in heat transfer properties and temperature distribution. The smooth tubes maintain a simplified flow profile (Figure 6(c)) with a uniform temperature distribution along the tube walls (Figure 7(c)), they peaked at consistent local Nusselt numbers (Figure 8(c)). In comparison, the presence of twisted tubes and tape inserts generate noticeable differences in fluid dynamics and heat transfer properties, confirming the effectiveness of these modifications in enhancing thermal performance.

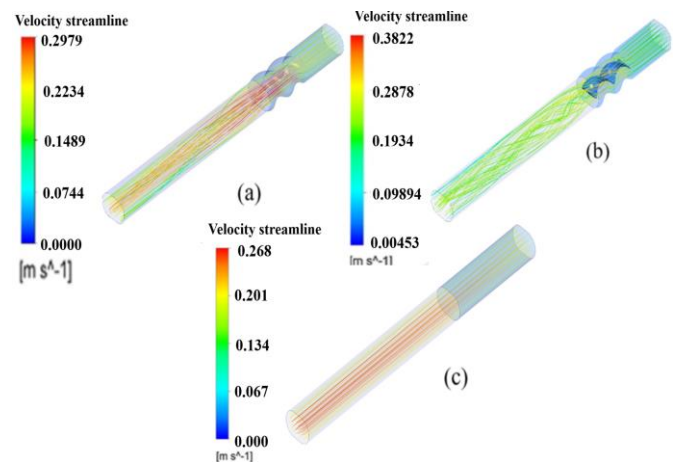


Figure 6. Comparison of streamlines for different types of tubes

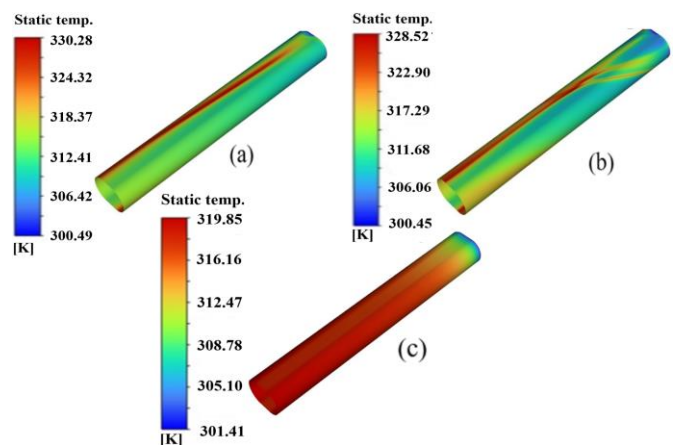
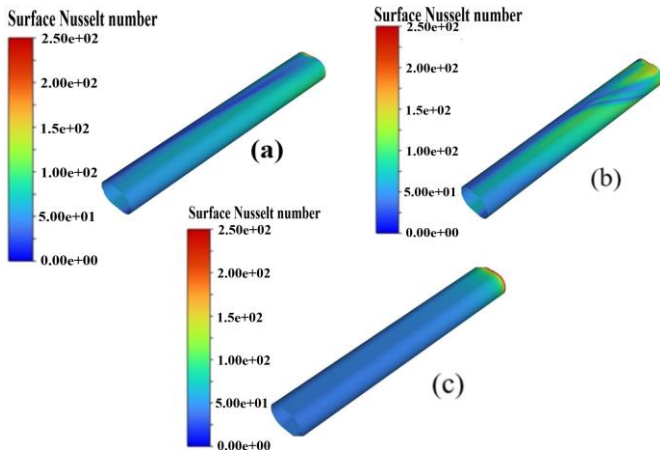


Figure 7. Comparison of temperature for different types of tubes



**Figure 8.** Comparison of local Nusselt number for different types of tubes

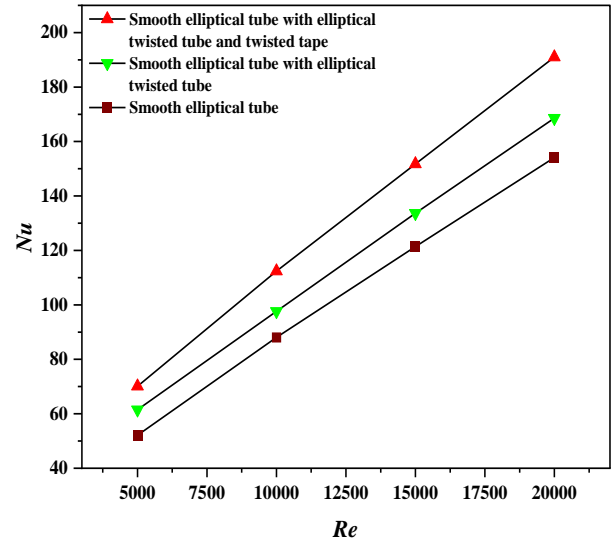
### 3.1.2 Effect on average Nusselt number and friction factor

Figure 9 and Figure 10 illustrate the influence of Reynolds number variations on the average Nusselt number and friction factor for different configurations: Smooth elliptical tube joined with elliptical twisted tubes and twisted tape insert, smooth elliptical tube joined with twisted tubes, and smooth tube alone. As depicted in Figure 9, an increase in the Reynolds number corresponds to an increase in the Nusselt number. Conversely, Figure 10 illustrates that the friction factor decreases as the Reynolds number increases.

The increase in average Nusselt number with increasing Reynolds number and the decrease in friction factor in turbulent flow can be attributed to the increased momentum transfer and enhanced mixing within the fluid. As Reynolds number increases in turbulent flow, the chaotic and swirling motion of the fluid intensifies. This turbulence disrupts the boundary layer, reducing its thickness and promoting greater mixing between the fluid layers. Consequently, the convective heat transfer coefficient increases, leading to higher average Nusselt numbers. Simultaneously, the increased momentum transfer within the turbulent boundary layer reduces the overall flow resistance. This results in lower friction factors, where viscous effects dominate. In turbulent flow, the turbulent fluctuations effectively mix momentum across the flow, reducing the overall resistance to flow.

Upon comparing the impact of tubes with twisted tubes, twisted tubes and tape inserts, and smooth tubes alone on the average Nusselt number and friction factor, noticeable trends become apparent. As observed in Figure 9, tubes with twisted tubes alone exhibit a moderate increase in average Nusselt numbers when compared to smooth tubes. This enhancement can be attributed to the intensified convective heat transfer resulting from the swirling motion. However, they also experience slightly higher friction factors due to increased flow resistance (Figure 10). In contrast, tubes with both twisted tubes and tape inserts exhibit further enhancements in average Nusselt numbers. The additional turbulence generated by the tape inserts intensifies heat transfer, resulting in even higher average Nusselt numbers than tubes with twisted tubes alone. However, this enhancement comes at the cost of higher friction factors compared to both twisted tubes alone and smooth tubes.

Smooth tubes, without any enhancements, generally have lower average Nusselt numbers due to their streamlined flow profile. However, they offer comparatively lower friction factors, as their flow profile experiences minimal disruptions.



**Figure 9.** Influence of Reynolds number variations on the average Nusselt number for different types of tubes

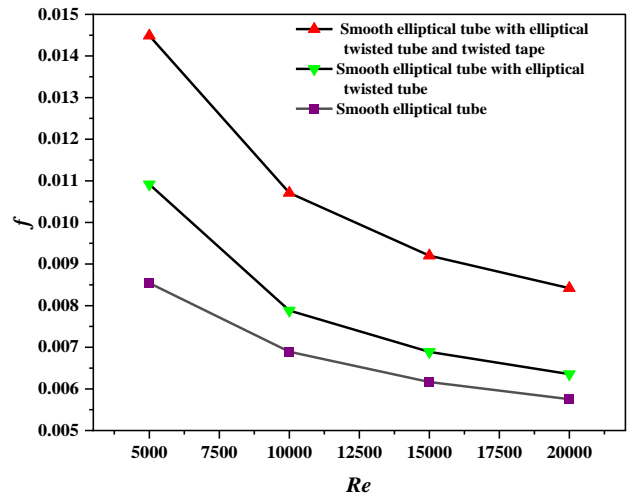


**Figure 10.** Influence of Reynolds number variations on the friction factor for different types of tubes

### 3.1.3 Effect on PEC

Evaluation of heat transfer enhancement through the use of twisted tube and twisted tape focuses on achieving the optimal balance between improved convective heat transfer and minimal increases in frictional losses. Engineers use Performance Evaluation Criteria (PEC) that compare the ratio of the average Nusselt number enhancement to the rise in friction factor.

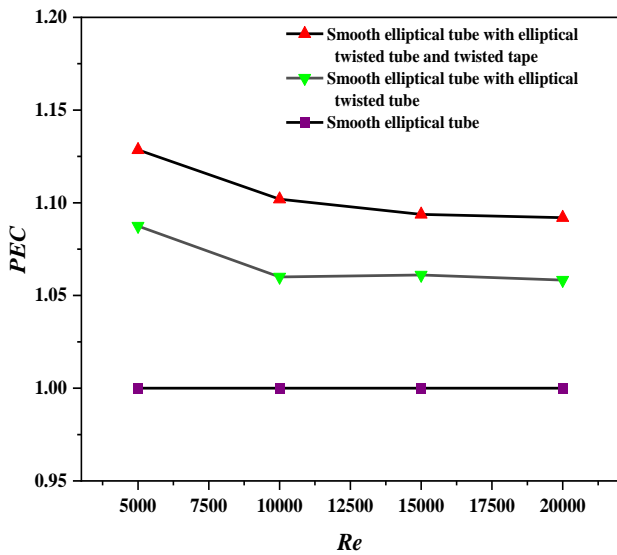
The Nusselt number measures the efficiency of convective heat transfer and serves as a critical parameter to determine the effectiveness of the heat exchanger. In contrast, the friction factor determines the energy loss due to resistance to fluid flow inside the pipe, which directly affects the pumping power requirement. By analyzing the ratio between these two parameters, engineers can determine the optimal compromise that maximizes heat transfer while maintaining reasonable levels of energy consumption associated with pumping.

Figure 11 shows that the thermohydraulic performance (PEC), characterized by the ratio of Nusselt number enhancement to increasing friction factor ( $Nu/f$ ), decreases with rising Reynolds numbers in smooth elliptical tubes associated with elliptical twisted tubes and twisted tape inserts,

as well as in elliptical tubes. Despite this decrease, the ratio remains above unity across the range studied, indicating a constantly intensifying effective heat transfer compared to the associated frictional buildup.

This downward trend can be attributed to the twisted tube and twisted tape giving rise to progressively greater turbulence and secondary flows at higher Reynolds numbers, which enhances heat transfer by disrupting the boundary layer but also causes increased shear stresses and pressure losses due to high velocity gradients and rotation. However, the  $Nu/f$  ratio remaining above one shows that the heat transfer enhancement effect still exceeds the frictional penalty.

Also, Figure 11 shows that the  $PEC$  values remain constant at higher Reynolds numbers, indicating fully developed flow. In this steady state condition, flow characteristics such as the velocity profile no longer change, indicating that the system has reached equilibrium.



**Figure 11.** Thermohydraulic performance ( $PEC$ ) vs variation of Reynolds numbers for different types of tubes

### 3.2 Effect of twisted pitch

This section investigates the impact of the twist pitch of the elliptical twisted tube with twisted tape inserts attached to the front of the elliptical plane tube on the Nusselt number and friction factor. A dimensional parameter called the degree of twisting has been introduced, denoted by  $P$ . All four twisted tube configurations share an identical cross-sectional geometry. The pitch values examined in this study are 0.1, 0.05, 0.033, and 0.025 m.

#### 3.2.1 Effect of twisted pitch on Nusselt number and friction factor

Figure 12, Figure 13 and Figure 14 illustrate the Nusselt number and friction factor for four distinct smooth elliptical tubes joined with twisted elliptical tubes and twisted tape inserts at varying twist pitch distances. These results are compared to those obtained from a smooth elliptical tube alone.

Analyzing Figure 12, it is clear that the Nusselt number demonstrates an approximately linear relationship with the Reynolds number. As the Reynolds number increases from 5000 to 20000, the Nusselt number also rises. Comparing the Nusselt numbers of the four smooth elliptical tubes joined with twisted elliptical tubes and twisted tape inserts, it becomes

clear that Case  $P=0.025$  m exhibits the highest Nusselt number, while Case  $P=0.1$  m demonstrates the lowest. Furthermore, in comparison to the smooth elliptical tubes without twisted elliptical tubes and twisted tape inserts, all the smooth elliptical tubes joined with twisted elliptical tubes and twisted tape inserts display higher Nusselt numbers. This can be attributed to the improved heat transfer capability of the twisted tubes relative to the smooth tube. Additionally, the discrepancy in the Nusselt number between the twisted tubes becomes more pronounced as the Reynolds number increases.

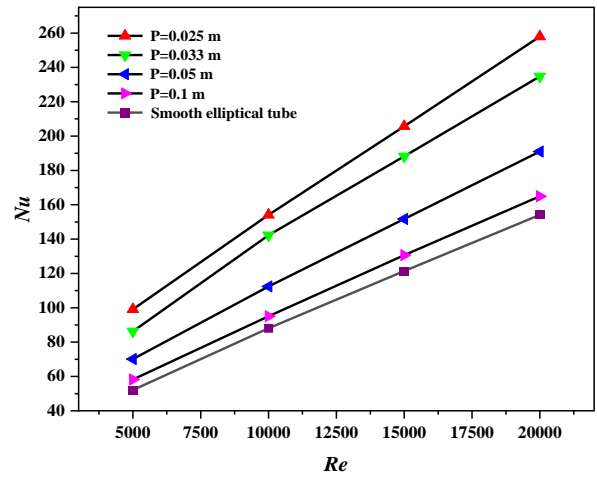


**Figure 12.** Influence of  $Re$  variations on the  $Nu$  for smooth elliptical tubes joined with twisted elliptical tubes and twisted tape inserts at varying twist pitch distances

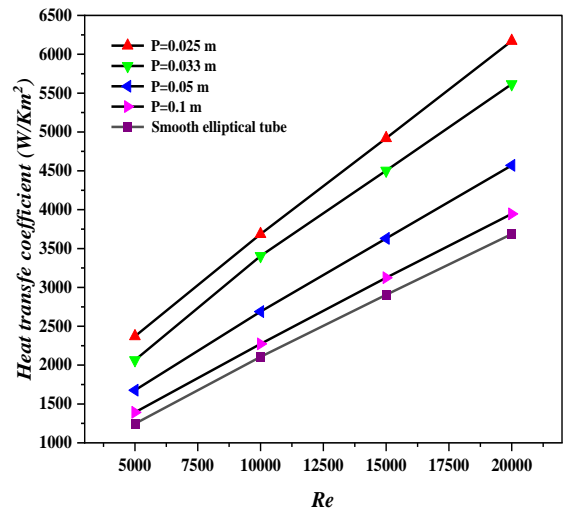


**Figure 13.** Influence of  $Re$  variations on the heat transfer coefficient for smooth elliptical tubes joined with twisted elliptical tubes and twisted tape inserts at varying twist pitch distances

Moving Figure 14 presents a comparison of the friction factor between the four studied smooth elliptical tubes joined with twisted elliptical tubes and twisted tape inserts at varying twist pitch and the smooth elliptical tube without twisted elliptical tubes and twisted tape inserts at various Reynolds numbers. The plotted data reveals that the friction factors decrease sharply as the Reynolds number increase from 5000 to 20000. Similar to the Nusselt number, a comparison of the friction factors of the twisted tubes reveals that Case  $P=0.025$  exhibits the highest value, while Case  $P=0.1$  m displays the



lowest value at the same Reynolds number.

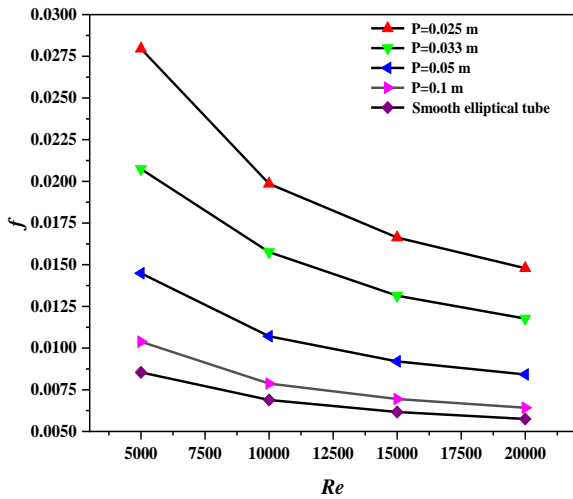


**Figure 14.** Influence of  $Re$  variations on the  $f$  for smooth elliptical tubes joined with twisted elliptical tubes and twisted tape inserts at varying twist pitch distances

When examining heat exchange, various aspects play a role, including piping configuration, inlet type and flow conditions, which are exemplified by the Reynolds number. Figure 13 delves into the effect of varying degrees of twist within the composite tube layout on the heat exchange coefficient across different Reynolds numbers. With increasing Reynolds numbers, the flow tends toward turbulence, which usually results in an improved heat exchange coefficient. Elliptical tubes with overlapping twists and tapes have proven remarkably effective in creating turbulence and secondary currents, disrupting the thermal boundary layer and enhancing heat exchange. This turbulence and secondary flow are important in increasing the thermal efficiency of the heat converter. For the most compact torsion pitch of 0.025 m, the design showed the highest heat exchange coefficient throughout the Reynolds number. The increased eddy current and rising turbulence resulting from the slightest twisting step dramatically increase heat exchange rates. But, this reinforcement is accompanied by an increased pressure drop due to expansion of frictional resistance, making it less suitable for contexts where pressure drop is a pressing concern. Average twist pitch of 0.033 m also shows improved heat exchange coefficients compared to smoother tubes but is less efficient than a twist pitch of 0.025 m. The balance between intense heat exchange and pressure taper is more favorable in this configuration, making it a potential contender for scenarios requiring moderate boosting free of excessive pressure confiscation. This balance makes it a versatile preference for diverse industrial applications.

The larger twisted pitch is 0.05 m and peaks at a lower heat exchange coefficient than smaller step but still exceeds the heat exchange coefficient of a neat elliptical tube. A lower number of twists results in lower turbulence, thus reducing heat exchange enhancement. This configuration may be suitable for scenarios where a moderate rise in heat exchange is sufficient, and alleviating the pressure drop is pivotal. The largest development pitch of 0.1 m showed the lowest heat exchange coefficient among the braided tubes.

The larger twist pitch generates less turbulence and swirling flow, resulting in a less significant enhancement of the heat transfer coefficient. This configuration might be more suitable

for applications where the pressure drop is a major concern, and only a slight improvement in heat transfer is needed.

Moreover, friction factors are consistently higher for all twisted tube configurations compared to the smooth tube benchmark. Decreasing the twist pitch of the twisted tube section and the twisted tape insert will impart greater swirling and tangential velocity to the flow. The lower twist pitch generates stronger vortex flows and secondary circulations. Near the inlet, the velocity profile will be more severely twisted and distorted. The higher swirl intensity will also persist further downstream before decaying. With the decreased twist pitch, the turbulence levels and turbulent mixing will be enhanced downstream. However, the lower twist pitch will also impose greater pressure losses due to increased friction. So an optimal twist pitch needs to be determined to obtain the desired heat transfer enhancement while minimizing pressure losses for the specific application. But overall, lower twisted tube and tape twist pitch impact the downstream flow in the smooth tube by inducing stronger twists and turbulence.

### 3.2.2 Effect on PEC

The impact of twist pitch on the heat transfer performance of smooth elliptical tubes joined with twisted elliptical tubes and twisted tape inserts was evaluated by examining the variations of the Performance Evaluation Criterion (PEC) at different Reynolds numbers, as depicted in Figure 15. It is evident from the plot in Figure 15 that the PEC of twisted tubes decreases as the twist pitch increases. This decline in PEC can be attributed to the reduction in the number of twists as the twist pitch increases, leading to a decrease in heat transfer quality and subsequently lowering the Nusselt number. The results in Figure 14 demonstrate that smaller twist pitches result in better heat transfer performance, with the peak heat transfer occurring at a Reynolds number of approximately 5000.

The highest PEC value, reaching 1.28, was observed in the twist pitch of 0.025 at a Reynolds number of 5000.

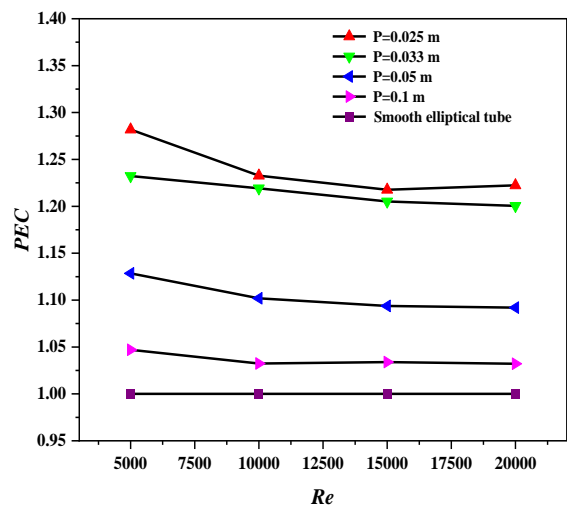


**Figure 15.** Influence of  $Re$  variations on the  $PEC$  for smooth elliptical tubes joined with twisted elliptical tubes and twisted tape inserts at varying twist pitch distances

## 4. CONCLUSION

This quantitative investigation delved into the analysis of heat transfer and fluid flow characteristics within an elliptical

tube featuring a twisted tube section and twisted tape inserts through the application of computational fluid dynamics. The research outcomes can be succinctly encapsulated as follows:

1. The incorporation of a twisted tube section and twisted tape inserts significantly boosts the efficacy of heat transfer in comparison to a plain elliptical tube, with the twisted configuration instigating swirling flow, turbulence, and enhanced thermal mixing.

2. Notably, the Nusselt number is augmented by 26.36% for the elliptical plain tube with twisted tube section coupled with twisted tape inserts, and 10.9% for the elliptical plain tube with twisted tube section alone, relative to the elliptical plain tube configuration. This substantial enhancement in heat transfer.

3. The smallest twist pitch of 0.025 m exhibits a remarkable 67.3% enhancement in the Nusselt number compared to the plain tube, coupled with a maximum performance evaluation criterion (PEC) value of 1.128. This configuration results in the highest heat transfer rates, albeit with a corresponding increase in pressure drop.

4. Friction factor analysis reveals a significant trade-off: while the twisted configurations substantially enhance heat transfer, they also lead to increased flow resistance. Specifically, the friction factor is augmented by 46.56% for the twisted tube section coupled with twisted tape inserts, and 14.62% for the twisted tube section alone, relative to the plain tube configuration.

It is imperative to identify an optimal twist pitch that strikes a balance between the desired enhancement in heat transfer and the accompanying pressure loss for a specific application.

Based on the paper's findings, the two most critical future work directions are:

1. **Multi-Objective Optimization:** Employ machine learning algorithms to optimize multiple parameters (twist pitch, tape thickness, tube cross-section) simultaneously, finding the ideal configuration that maximizes heat transfer while minimizing pressure drop. This is crucial because while the study showed significant heat transfer enhancements (up to 67.3% in Nusselt number), it also revealed substantial increases in friction factor (up to 46.56%), indicating a need to find the optimal balance between these competing objectives.

2. **Scale-Up Studies:** Conduct large-scale experiments to validate the CFD results and assess how the performance scales in industrial-sized heat exchangers. This is essential because while the study's numerical simulations show promising results, such as a maximum PEC value of 1.128 for the smallest twist pitch, these findings need to be verified in real-world, large-scale applications to ensure that the enhanced heat transfer and increased pressure drop characteristics are maintained at industrial scales.

## REFERENCES

[1] Churchill, S.W. (2003). Compact heat exchangers as chemical reactors. *Compact Heat Exchangers and Enhancement Technology for the Process Industries-2003*. Begel House Inc..

[2] Kabeyi, M.J.B., Olanrewaju, O.A. (2022). Sustainable energy transition for renewable and low carbon grid electricity generation and supply. *Frontiers in Energy Research*, 9: 743114. <https://doi.org/10.3389/fenrg.2021.743114>

[3] Zhou, J.Z., Jia, S.B. (2019). Development of a elliptic heat pipe heat exchanger. *Heat Pipe Technology:*

Volume 2, Materials and Applications, Begell House. <http://doi.org/10.1615/IHPC1990v2.410>

[4] Lopata, S., Oclon, P., Stelmach, T., Markowski, P. (2019). Heat transfer coefficient in elliptical tube at the constant heat flux. *Thermal Science*, 23(Suppl. 4): 1323-1332. <https://doi.org/10.2298/TSCI19S4323L>

[5] Cheng, J., Qian, Z., Wang, Q., Fei, C., Huang, W. (2019). Numerical study of heat transfer and flow characteristic of twisted tube with different cross section shapes. *Heat and Mass Transfer*, 55: 823-844. <https://doi.org/10.1007/s00231-018-2471-7>

[6] Mushatet, K.S. (2023). A review study for a twisted tube heat exchanger. *Journal of Nanofluids*, 12(2): 299-317. <https://doi.org/10.1166/jon.2023.1926>

[7] Alempour, S.M., Abbasian Arani, A.A., Najafizadeh, M.M. (2020). Numerical investigation of nanofluid flow characteristics and heat transfer inside a twisted tube with elliptic cross section. *Journal of Thermal Analysis and Calorimetry*, 140(3): 1237-1257. <https://doi.org/10.1007/s10973-020-09337-z>

[8] Xiao, K., He, J., Feng, Z. (2022). Heat transfer enhancement of swirl cooling by different crossflow diverters. In *Turbo Expo: Power for Land, Sea, and Air*, 86045: V06BT15A023. <https://doi.org/10.1115/GT2022-82775>

[9] Luan, Y., Rao, Y., Wang, K., Wu, W. (2022). Experimental and numerical study of heat transfer and pressure loss in a swirl multi-pass channel with convergent jet slots. *Journal of Turbomachinery*, 144(7): 071006. <https://doi.org/10.1115/1.4053487>

[10] Uyanık, M., Dağdevir, T., Özceyhan, V. (2022). Thermo-hydraulic performance investigation of a heat exchanger tube inserted with twisted tapes modified with various twist ratio and alternate axis. *European Mechanical Science*, 6(3): 189-195. <https://doi.org/10.26701/ems.1032081>

[11] Samruaisin, P., Kunlabud, S., Kunnarak, K., Chuwattanakul, V., Eiamsa-Ard, S. (2019). Intensification of convective heat transfer and heat exchanger performance by the combined influence of a twisted tube and twisted tape. *Case Studies in Thermal Engineering*, 14: 100489. <https://doi.org/10.1016/j.csite.2019.100489>

[12] Indurain, B., Uystepuyst, D., Beaubert, F., Lalot, S., Helgadóttir, Á. (2020). Numerical investigation of several twisted tubes with non-conventional tube cross sections on heat transfer and pressure drop. *Journal of Thermal Analysis and Calorimetry*, 140: 1555-1568. <https://doi.org/10.1007/s10973-019-08965-4>

[13] Zhao, J., Li, L., Xie, W., Zhao, H. (2022). Flow and heat transfer characteristics of liquid metal and supercritical CO<sub>2</sub> in a twisted tube heat exchanger. *International Journal of Thermal Sciences*, 174: 107453. <https://doi.org/10.1016/j.ijthermalsci.2021.107453>

[14] Luo, C., Song, K., Tagawa, T., Liu, T. (2020). Heat transfer enhancement in a novel annular tube with outer straight and inner twisted oval tubes. *Symmetry*, 12(8), 1213. <https://doi.org/10.3390/sym12081213>

[15] Mushatet, K.S., Rishak, Q.A., Fagr, M.H. (2020). Experimental and numerical investigation of swirling turbulent flow and heat transfer due to insertion of twisted tapes of new models in a heated tube. *Applied Thermal Engineering*, 171: 115070. <https://doi.org/10.1016/j.applthermaleng.2020.115070>

- [16] Tusar, M., Ahmed, K., Bhuiya, M., Bhowmik, P., Rasul, M., Ashwath, N. (2019). CFD study of heat transfer enhancement and fluid flow characteristics of laminar flow through tube with helical screw tape insert. *Energy Procedia*, 160: 699-706. <https://doi.org/10.1016/j.egypro.2019.02.188>
- [17] Outokesh, M., Ajarostaghi, S.S.M., Bozorgzadeh, A., Sedighi, K. (2020). Numerical evaluation of the effect of utilizing twisted tape with curved profile as a turbulator on heat transfer enhancement in a pipe. *Journal of Thermal Analysis and Calorimetry*, 140: 1537-1553. <https://doi.org/10.1007/s10973-020-09336-0>
- [18] Alzahrani, S., Usman, S. (2019). CFD simulations of the effect of in-tube twisted tape design on heat transfer and pressure drop in natural circulation. *Thermal Science and Engineering Progress*, 11: 325-333. <https://doi.org/10.1016/j.tsep.2019.03.017>
- [19] Aslan, E., Ozsaban, M., Ozcelik, G., Guven, H.R. (2021). A numerical analysis of convection heat transfer and friction factor for oscillating corrugated channel flows. *Heat Transfer Engineering*, 42(3-4): 181-190. <https://doi.org/10.1080/01457632.2019.1699287>
- [20] Talebi, M., Lalgani, F. (2021). Assessment of thermal behavior of variable step twist in the elliptical spiral tube heat exchanger. *International Journal of Thermal Sciences*, 170: 107126. <https://doi.org/10.1016/j.ijthermalsci.2021.107126>
- [21] Ahmed, M.A., Yusoff, M.Z., Ng, K.C., Shuaib, N.H. (2014). Effect of corrugation profile on the thermal-hydraulic performance of corrugated channels using CuO-water nanofluid. *Case Studies in Thermal Engineering*, 4: 65-75. <https://doi.org/10.1016/j.csite.2014.07.001>